Coordinated Particle Relocation Using Finite Static Friction with Boundary Walls

Arne Schmidt[1], Victor M. Baez[2], Aaron T. Becker[2] and Sándor P. Fekete[1]

***Abstract*—We present theoretical and practical methods for achieving *arbitrary* reconfiguration of a set of objects, based on the use of external forces, such as a magnetic field or gravity: Upon actuation, each object is pushed in the same direction until it collides with an obstruction. This concept can be used for a wide range of applications in which particles do not have their own energy supply.**

A crucial challenge for achieving any desired target configuration is breaking global symmetry in a controlled fashion. Previous work made use of specifically placed barriers; however, introducing precisely located obstacles into the workspace is impractical for many scenarios. In this paper, we present a different, less intrusive method: making use of the interplay between static friction with a boundary and the external force to achieve arbitrary reconfiguration. Our key contributions are a precise *theoretical* characterization of the critical coefficient of friction that is sufficient for rearranging two particles in triangles, convex polygons, and regular polygons; a method for reconfiguring multiple particles in rectangular workspaces, and deriving *practical* algorithms for these rearrangements. Hardware experiments show the efficacy of these procedures, demonstrating the usefulness of this novel approach.

***Index Terms*—Manipulation Planning, Underactuated Robots**

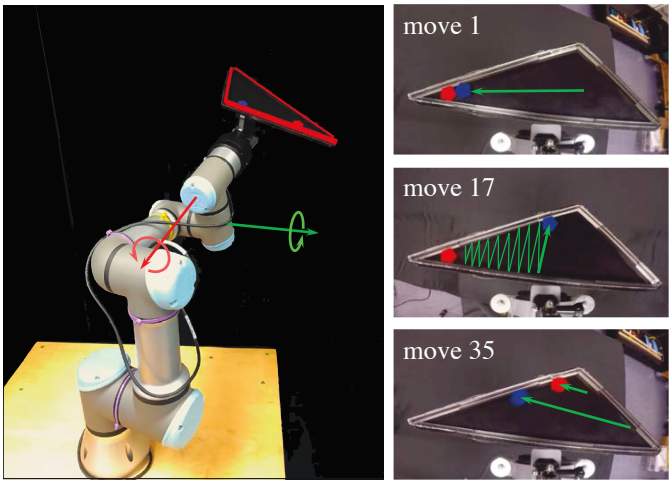

Fig. 1. (Left) Using a robotic apparatus to impose a global force on a configuration of particles. (Right) A reconfiguration sequence that combines global force and local friction to achieve arbitrary repositioning of particles.

I. Introduction

RECONFIGURING a large set of objects in a prespecified manner is a fundamental task for a large spectrum of applications, including swarm robotics, smart materials and advanced manufacturing. In many of these scenarios, the involved items are not equipped with individual motors or energy supplies, so actuation must be performed from the outside. Moreover, reaching into the workspace to manipulate individual particles of an arrangement is often impractical or even impossible; instead, global external forces (such as gravity or a magnetic force) may be have to employed, targeting each object in the same, uniform manner. These limitations of individual navigation apply even in scenarios of swarm robotics: For example, the well-known kilobots do have individual actuation and energy supply, but often make use of an external light source for navigation [14]; as a consequence, directing a swarm of kilobots by switching on a light beacon works just like activating an external force. This concept of global control has also been studied for using biological cells as reactive robots controlled by magnetic fields, see Arbuckle and Requicha [3] and Kim et al. [10]. Global control also has applications in assembling nano- and micro-structures. Related work shows how to assemble shapes by adding one particle at a time [7], [4], or combining multiple pairs of subassemblies in parallel in one time step [16].

Considering this approach of navigation by a global external force gives rise to a number of problems, including navigation of one particle from a start to a goal position [11], particle computation [5], [6], or emptying a polygon [2]. Zhang et al. [19], [20] show how to rearrange a rectangle of agents in a workspace that is only constant times larger than the number of agents. Akella et al. [1] consider the problem of reconfiguring an object on a conveyor belt with a simple robot, and Lynch et al. [12] use a mobile robot with a flat pusher plate as the gripper to manipulate objects.

A crucial issue for all these tasks is how to combine the use of a uniform force (which is the same for all involved items) with the individual requirements of object relocation (which may be distinct for different particles): How can we achieve an *arbitrary* arrangement of particles if all of them are subjected to the same external force? Previous work (such as [6]) has shown how arbitrary reconfiguration of an ensemble is possible with the help of specifically placed barriers; however, introducing precisely located obstacles into the workspace is impractical for many scenarios. In this paper, we present a different, less intrusive method: making use of the interplay

Manuscript received: Sept. 19, 2019; Revised Dec. 10, 2019; Accepted Jan. 7, 2020.

This paper was recommended for publication by Editor Dezhen Song upon evaluation of the Associate Editor and Reviewers' comments.

[1]Department of Computer Science, TU Braunschweig, 38106 Braunschweig, Germany {s.fekete, arne.schmidt}@tu-bs.de

[2]Department of Electrical & Computer Engineering, University of Houston, USA. This work was supported by National Science Foundation IIS-1553063 and IIS-1619278. {vjmontan, atbecker}@uh.edu

Digital Object Identifier (DOI): see top of this page.

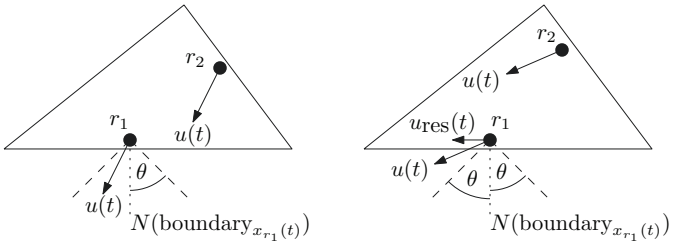

Fig. 2. Left: An input force command $u(t)$ within the cone $\pm\theta$ about the normal to the boundary results in no motion of r_1. Right: An input force command $u(t)$ outside the cone results in a motion of both particles. Observe that r_1 slides along the boundary with a resulting force $u_{\text{res}}(t)$.

between static friction with a boundary of the workspace and the external force to achieve any desired configuration.

A. Our Results.

We provide a fundamentally new approach to manipulating a swarm of objects by an external, global force, demonstrating how static boundary friction can be employed to achieve arbitrary reconfiguration. Our results include the following.

- We show that any two particles in an arrangement can be arbitrarily relocated in a triangle, provided sufficient friction as a function of the triangle geometry.
- More specifically, for a triangle with second smallest angle β, we prove that an angle of friction of $\frac{\pi}{2} - \beta$ is sometimes necessary and always sufficient to guarantee any reconfiguration.
- We also provide procedures for reconfiguring more than two particles, including sorting a line of n particles.
- We provide hardware experiments showing the efficacy of our strategies, as illustrated in Fig. 1.

B. Other Related Work.

Sliding a component using an active tilting tray has a rich history, especially on sensorless part orientation, see [8], [13]. Similar work also applies to using sliding-jaw grippers with low-friction contact surfaces to localize parts without sensing [9]. Shahrokhi et al. [17], [18] considered reconfiguration problems of particles using friction at the walls. However, they assume walls have infinite friction, i.e., a particle lying at a wall cannot be moved when there is a movement parallel to the wall. This differs from the more realistic assumptions in this paper, in which we only consider finite friction. For a theoretical investigation of friction-less sliding tile particles moving on a 2D grid in the presence of obstacles, see the recent paper by Balanza-Martinez et al. [4] and its bibliography.

II. Preliminaries

The *coefficient of friction* is a property of the surfaces of any two materials brought in contact. The coefficient of friction is a ratio of the force required to move a surface horizontally past another and the force with which the materials are pressed together. If a particle is placed on a flat plate that is tilted until the object slides, the tangent of the angle when the sliding commences is the coefficient of friction.

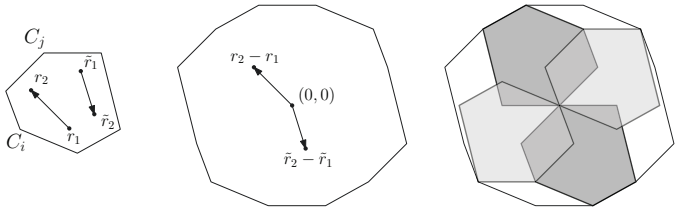

Fig. 3. Left: A six-sided polygon P with start positions r_1 and r_2 for two particles and their goal positions $\tilde{r}_1$ and $\tilde{r}_2$. Middle: The Δ configuration of the polygon and the positions of the start and end configuration. Right: Lightgray (darkgray) area corresponds to the C_i-area (C_j-area, resp.).

Definition 1. *Let θ be the* angle of friction *and $\mu := \tan\theta$ be the* coefficient of friction.

See Fig. 2 for an illustration. For a particle r, let $\mathrm{N}(\text{boundary}_{\mathrm{x}_r(t)})$ be the normal to the boundary at position $\mathrm{x}_r(t)$. For notational simplicity, we also use r as the position of the particle. For a force command $\mathrm{u}(t)$, if a particle r has position $\mathrm{x}_r(t)$ and velocity $\dot{\mathrm{x}}_r(t)$ at time t, we assume the following, where $\alpha = \arccos(\mathrm{u}(t) \cdot \mathrm{N}(\text{boundary}_{\mathrm{x}_r(t)}))$ if r lies on the boundary:

$$\dot{\mathrm{x}}_r(t) = \begin{cases} 0, & \text{if } \mathrm{x}_r(t) \in \text{boundary} \\ & \textbf{and } \alpha \le \theta, \\ c_k \|\mathrm{u}(t)\| \cdot \sin\alpha, & \text{if } \mathrm{x}_r(t) \in \text{boundary} \\ & \textbf{and } \frac{\pi}{2} \ge \alpha > \theta, \\ \|\mathrm{u}(t)\|, & \text{otherwise,} \end{cases}$$

where $c_k < 1$ is some coefficient depending on the kinetic friction. Throughout this paper, we will only consider the first and the third case, i.e., each particle moves at full speed or does not move at all.

Problem 1. *Given a* workspace*, i.e., a convex polygon with n vertices $v_1, \ldots, v_n$, with m particles $r_1, \ldots, r_m$, and an angle of friction θ. Is it possible to reach the configuration $\tilde{r}_1, \ldots, \tilde{r}_m$?*

In this paper, we do not make any assumption on the initial positions of $r_1, \ldots, r_m$, except that all particles are well separated, i.e., they have a distance $\varepsilon > 0$ to each other.

Definition 2 (Δ Configuration)**.** *The Δ configuration space Δ_P of a convex polygon P containing two particles is a polygon obtained by translating n copies of P, such that each vertex of P is moved to the origin, and taking the convex hull of all copies (for an example see Figure 3).*

We observe that Δ_P can also be defined by taking the convex hull of differences between each pair of vertices. More formally:

$$\Delta_P := \mathrm{ch}\left(C_i - C_j \mid C_i, C_j \in P\right),$$

where $\mathrm{ch}(\cdot)$ denotes the convex hull. From this alternative definition follows that $\Delta_P = \Delta_{-P}$, where $-P$ is P rotated by π. This motivates the following definition.

Definition 3. *Let P be a convex polygon and v be a vertex in P. A v-area in Δ_P is the union of P and $-P$ having v centered at the origin (see Figure 3 right).*

Note that the union of v-areas for all $v \in P$ equals Δ_P.

III. Reconfiguration of Two Particles

Just like in the context of sorting algorithms in computer science or discrete mathematics, a critical component for achieving arbitrary reconfiguration of larger ensembles is the ability to rearrange two specific particles. For our purposes of employing external forces and static friction, the additional aspects of geometry and physics have to be considered. These are addressed in this section, before we proceed to show how this can be generalized to large ensembles in the next section.

The main idea for this first step is to try to completely cover the Δ configuration. We start by developing a strategy for separating two particles in Subsection A, which gives us a lower bound for θ for every strategy in this section. This is followed by an upper bound for θ in triangles (Subsection B) and arbitrary convex polygons (Subsection C), i.e., we can guarantee any reconfiguration with any angle of friction higher than this upper bound.

A. Separating two particles

As a first step, we show how to separate two specific particles.

Lemma 1. *Assume particle r_1 is positioned in a corner with angle α, then we can move r_2 to any position in the polygon without moving r_1, if $\mu > \tan(\frac{\alpha}{2})$, i.e., the angle of friction is greater than $\frac{\alpha}{2}$.*

Proof. We perform a zig-zag move (Figure 5(a) left) that increases the distance between r_1 and r_2. Consider Figure 4. W.l.o.g., r_1 sits in the corner bounded by segments s_1 and s_2, while r_2 starts on segment s_1 with distance c to r_1. We move r_2 to the other segment s_2 with the maximum angle possible. Particle r_2 reaches s_2 with distance b to r_1. Afterwards, we move r_2 back to s_1, now having a distance of c'. If θ is sufficiently large, then $c' > c$.

For a given θ, we have

$$b = c \cdot \frac{\sin(\frac{\pi}{2} - \alpha + \theta)}{\sin(\frac{\pi}{2} - \theta)} = c \cdot \frac{\cos(\theta - \alpha)}{\cos(\theta)},$$

and therefore

$$c' = c \cdot \frac{\cos^2(\theta - \alpha)}{\cos^2(\theta)}.$$

If $c' > c$, then $\cos^2(\theta - \alpha) > \cos^2(\theta)$. This is true if $\cos(\theta - \alpha) > \cos(\theta)$. By applying the $\arccos$ function, this yields $\alpha - \theta < \theta$, if $\theta < \alpha$, and $\theta - \alpha < \theta$, if $\theta \geq \alpha$. The first case is true iff $\theta > \frac{\alpha}{2}$, the second case is always true for $\alpha > 0$. Hence, for $\theta > \frac{\alpha}{2}$ we can increase the distance between r_1 and r_2. By moving r_2 by short movements, we can relocate r_2 to any corner of a given polygon. Note that if α is an obtuse angle, the same formula can be derived. □

Note that in a triangle an angle of friction of $\frac{\alpha}{2}$ is necessary.

B. Reconfiguration of two particles in arbitrary triangles

Let T be a triangle and let A, B and C be the corners with angles α, β and γ. Furthermore, let α be the smallest angle in T and we assume that $\theta > \frac{\alpha}{2}$ is guaranteed. Consider two

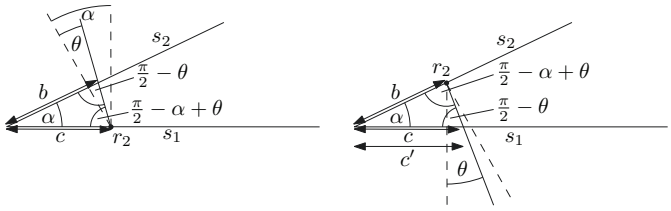

Fig. 4. A corner of a polygon with angle α. Left: r_2 lies on s_1 and is moved to s_2. Right: r_2 is moved back to s_1. r_2 can be moved away from the corner if the angle of friction exceeds $\frac{\alpha}{2}$

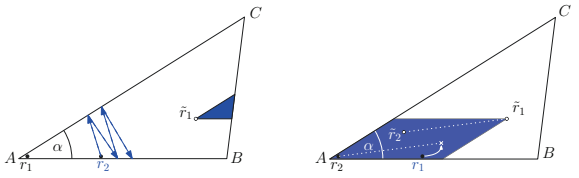

(a) Blue strategy. Dotted lines represent the vector $\tilde{r}_2 - \tilde{r}_1$

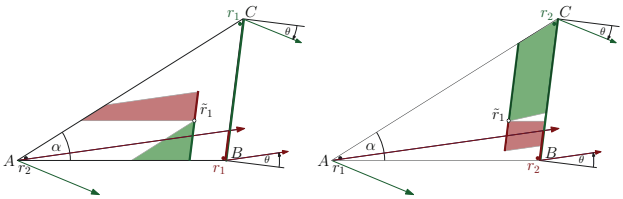

(b) Red and green strategy

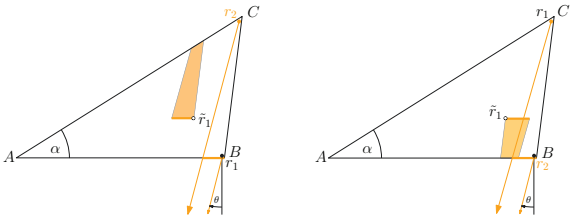

(c) Orange strategy

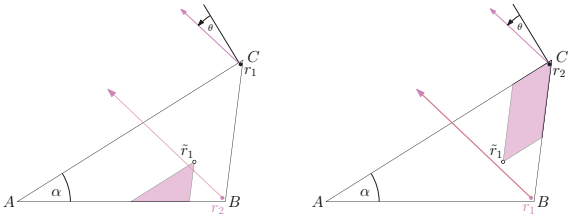

(d) Violet strategy

Fig. 5. Illustration of the five strategies. Colored areas correspond to valid goal positions for r_2, if the goal position of r_1 is $\tilde{r}_1$. Left column: We fix r_1 and move r_2. Right column: We switch intermediate locations of r_1 and r_2.

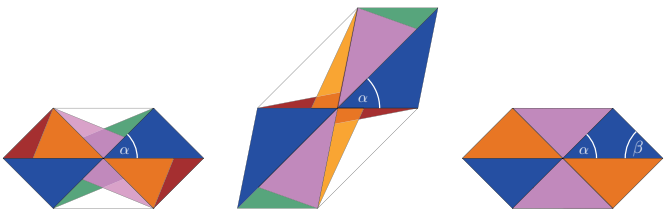

(a) (b) (c)

Fig. 6. Shown in (a) and (b) are the Δ configurations of the blue triangle. Both blue triangles correspond to the A-area. Colors represent the areas in the Δ configuration covered by our five strategies with an angle of friction of $\frac{\alpha}{2} + \varepsilon$ for some $\varepsilon > 0$. (a),(b): We observe that every strategy may cover areas not covered by any other strategy. (c): If $\theta > \frac{\pi}{2} - \beta$ then we can guarantee full coverage.

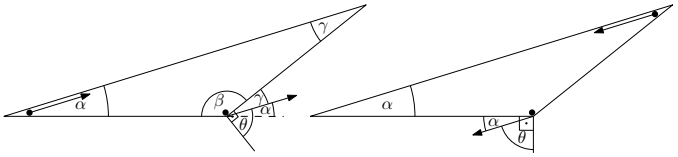

Fig. 7. Left: Computation of minimum θ needed for the red strategy. Right: Computation of minimum θ needed for the final step of the orange strategy.

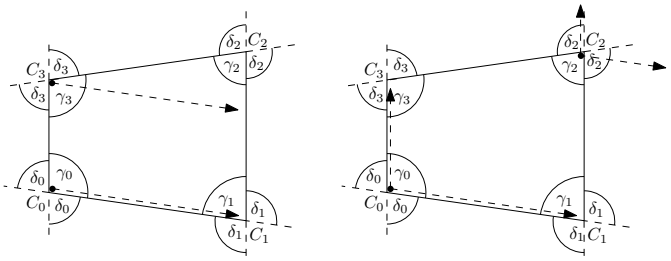

Fig. 8. Left: If we want to move a particle in C_0 without moving a particle in C_3, some movements are prohibited (even if we have infinite friction), because $\delta_0 < \gamma_3$. Right: However, we can move the particle in C_0 to any place in the polygon without moving a particle in C_2 (unless the friction is too small), because $\delta_3 + \delta_0 > \gamma_2$ and $\delta_1 + \delta_0 > \gamma_2$.

particles r_1 and r_2 within a triangle and their goal positions $\tilde{r}_1$ and $\tilde{r}_2$. We have the following strategies to reach the goal positions (see also Fig. 5 for a graphical sketch):

Blue: Move r_1 to A. As in Lemma 1, use zig-zag moves to place r_2 in T while r_1 is fixed in A, such that $r_2 - r_1 = \tilde{r}_2 - \tilde{r}_1$. Then, translate r_1 and r_2 to their goal positions.

Red: First, place r_2 in A and move r_1 to B. Then, place r_2 anywhere in the area spanned by $\overline{AB}$ and the angle of friction θ. Afterwards, translate r_1 and r_2 to their goal positions.

Green: First, Place r_2 in A and move r_1 to C. Then, place r_2 in the area spanned by $\overline{AC}$ and the angle of friction θ, such that $r_2 - r_1 = \tilde{r}_2 - \tilde{r}_1$. Afterwards, translate r_1 and r_2 to their goal positions.

Orange: Place r_2 in C and r_1 in B (as we will see later, this is always possible if $\theta > \frac{\alpha}{2}$; see Theorem 2). Then, place r_2 in the area spanned by $\overline{BC}$ and the angle of friction, such that $r_2 - r_1 = \tilde{r}_2 - \tilde{r}_1$. Afterwards, translate both particles to their goal position.

Violet: Place r_2 in B and r_1 in C. Then, place r_2 anywhere in the area spanned by $\overline{CB}$ and the angle of friction, such that $r_2 - r_1 = \tilde{r}_2 - \tilde{r}_1$ Finally, translate both particles to their goal position.

These strategies can also be used by switching the particles r_1 and r_2. Assume that r_1 lies in corner A. To switch r_1 and r_2, we separate both particles to corners B and C, then we use strategy orange or violet (depending on which particle is in which corner), and as a last step, we move r_2 to A.

Observation 1. *In the Δ configuration, the only strategies that overlap are red with orange and green with violet.*

Furthermore, the blue strategy fills out the A-area completely, red and orange fill out parts of the B-area, and green and violet fill out parts of the C-area

Lemma 2. *If $\theta > \frac{\pi}{2} - \gamma$, then the area of the red and orange strategy covers the B-area completely.*

Proof. W.l.o.g., assume that $\alpha \leq \beta \leq \gamma$. First observe that, if the B-area is covered, then the red or the orange strategy covers the area on its own. Therefore, we search for the minimum angle needed such that one of the two strategies covers the B-area.

Red strategy: Red covers the B-area if we can move r_1 (r_2, resp.) to C without moving r_2 (r_1, resp.). To this end, the angle of friction must be $\frac{\pi}{2} - \gamma$ (see Figure 7 left).

Orange strategy: Assume that r_1 and r_2 already lie in B and C, respectively. To cover the B-area, r_2 must be movable to A without moving r_1. This requires an angle of friction of at least $\frac{\pi}{2} - \alpha$.

Because $\alpha \leq \gamma$, we only need to consider the red strategy for full coverage and thus, $\theta > \frac{\pi}{2} - \gamma$ is sufficient to cover the B-area. □

Lemma 3. *If $\theta > \frac{\pi}{2} - \beta$, then the area of the green and violet strategy covers the C-area completely.*

Proof. The argument of the previous lemma applies. □

Theorem 1. *Let T be a triangle with angles $\alpha \leq \beta \leq \gamma$. If $\theta > \frac{\pi}{2} - \beta$, then we can guarantee any reconfiguration of two particles, i.e., Δ_T is completely covered by our strategies.*

Proof. To cover the A-, B-, and C-area of the Δ configuration, the angle of friction θ must be greater than $\max(\frac{\alpha}{2}, \frac{\pi}{2} - \beta, \frac{\pi}{2} - \gamma)$. Because $\beta \leq \gamma$ we have that $\frac{\pi}{2} - \beta \geq \frac{\pi}{2} - \gamma$.

We can rewrite $\frac{\pi}{2} - \beta$ as $\frac{\pi - 2\beta}{2} = \frac{\alpha + \gamma - \beta}{2} \geq \frac{\alpha}{2}$ (because $\gamma - \beta \geq 0$). Therefore, an angle of friction of at least $\frac{\pi}{2} - \beta$ guarantees full coverage of Δ_T. □

With the following theorem we show that, if θ is slightly larger than $\frac{\alpha}{2}$, then we can guarantee two thirds of all reconfigurations. Furthermore, the proof implies that two particles can be separated to B and C for any $\theta > \frac{\alpha}{2}$.

Theorem 2. *For a triangle T with angles $\alpha \leq \beta \leq \gamma$, at least two thirds of all configurations can be guaranteed if $\theta > \frac{\alpha}{2}$.*

Proof. Following Lemma 2, we need an angle of friction of at least $\frac{\pi}{2} - \gamma$ to cover the B-area. Because $\frac{\pi}{2} - \gamma = \frac{\pi - 2\gamma}{2} \leq \frac{\pi - \gamma - \beta}{2} = \frac{\alpha}{2}$, the B-area is always covered if $\theta > \frac{\alpha}{2}$. Furthermore, the A-area (covered by the blue strategy) and the B-area are two thirds of Δ_T, and thus, we can guarantee two thirds of all possible configurations. □

C. Reconfiguration of two particles in convex polygons

Now we proceed to develop strategies to reconfigure two particles in convex polygons by generalizing the strategies for triangles, i.e., for a particle r_1 in corner C_i and a particle r_2 in corner C_j, moving particle r_2 to cover the C_i-area. As shown in Figure 8, we cannot guarantee full coverage with this strategy, because any movement for r_2 in direction to C_1 would also move r_1. This happens for all pairs of vertices (C_i, C_j) of P, where the segment C_jC_{j+1} has a larger negative slope than the segment C_iC_{i-1}.

Definition 4. *For a vertex $C_i \in P$, let δ_i be the exterior angle at vertex C_i. Let $P^+_{i,j} := \{C_i, C_{i+1}, \dots, C_{j-1}, C_j\}$ and $P^-_{i,j} := \{C_i, C_{i-1}, \dots, C_{j+1}, C_j\}$.*

Furthermore, let $P_i := \{C_j \in P \mid \sum_{C_k \in P^+_{i+1,j}} \delta_k \geq \gamma_i \wedge \sum_{C_k \in P^-_{i-1,j}} \delta_k \geq \gamma_i\}$, i.e., P_i contains every vertex of P such that we can use the strategy described in the beginning of this section. Note that all indices are modulo n.

Lemma 4. *For a vertex C_i of P, we have $|P_i| \geq 1$.*

Proof. Assume that $|P_i| = 0$. Then, there are two adjacent vertices C_j and $C_{j'}$ such that $\sum_{C_k \in P^+_{i+1,j}} \delta_k < \gamma_i$ and $\sum_{C_k \in P^-_{i-1,j'}} \delta_k < \gamma_i$. This implies that $2\gamma_i > \sum_{C_k \in P^+_{i+1,j}} \delta_k + \sum_{C_k \in P^-_{i-1,j'}} \delta_k = -\delta_i + \sum_{C_k \in P} \delta_k = -\delta_i + 2\pi > 2\pi - 2\delta_i = 2\gamma_i$. This is a contradiction and therefore $|P_i| \geq 1$. □

Lemma 5. *Let P be a convex polygon with vertices $C_0, \dots, C_{n-1}$ and angles $\gamma_0, \dots, \gamma_{n-1}$. We can cover the C_i-area if $\theta > \min_{j \in P_i} \left(\frac{\gamma_i}{2}, \max\left(\frac{\gamma_j}{2}, \eta^+_{i,j} - \frac{\pi}{2}, \eta^-_{i,j} - \frac{\pi}{2}\right)\right)$, where $\eta^+_{i,j} := \sum_{C_k \in P^+_{i+1,j-1}} \delta_k$ and $\eta^-_{i,j} := \sum_{C_k \in P^-_{i-1,j+1}} \delta_k$.*

Proof. We consider two strategies to cover the C_i-area. The first strategy keeps one particle in the corner C_i and moves the second particle to any position in the polygon. This requires an angle of friction of more than $\frac{\gamma_i}{2}$.

The second strategy picks one vertex $C_j \in P_i$ and proceeds in two steps. See Fig. 9 for an illustration. In step one, one particle is kept in corner C_j while the other particle is moved to corner C_i. This requires an angle of friction of more than $\frac{\gamma_j}{2}$. In step two, we move the particle from corner C_j to any place in the polygon. We show that an angle of friction of $\max(\eta^+_{i,j} - \frac{\pi}{2}, \eta^-_{i,j} - \frac{\pi}{2})$ is sufficient to do this.

The segment C_iC_j splits the polygon into subpolygons, i.e., $P^+_{i,j}$ and $P^-_{i,j}$, and splits the angle γ_i (γ_j) into two angles γ_i^+ and γ_i^- (γ_j^+ and γ_j^-). W.l.o.g., consider $P^+_{i,j}$ (calculations for $P^-_{i,j}$ are analogous). To move the particle, say r_1, from C_j anywhere in $P^+_{i,j}$, it must be possible to move r_1 in direction $\vec{v} = C_{j-1} - C_j$ without moving the particle in C_i. Therefore, θ must be at least the angle that is enclosed by $\vec{v}$ and the orthogonal of the segment $s := \overline{C_iC_{i+1}}$. We observe that the angle between $\vec{v}$ and s is $\pi - \gamma_i^+ - \gamma_j^+$. The sum $\gamma_i^+ + \gamma_j^+$ can be calculated by taking the sum of angles in $P^+_{i,j}$ and subtract every angle of $P^+_{i,j}$ except γ_i^+ and γ_j^+. More formal: $\gamma_i^+ + \gamma_j^+ = (|P^+_{i,j}| - 2)\pi - \sum_{C_k \in P^+_{i+1,j-1}} \gamma_k = \sum_{C_k \in P^+_{i+1,j-1}} \pi - \gamma_k = \sum_{C_k \in P^+_{i+1,j-1}} \delta_k = \eta^+_{i,j}$. Because the angle between $\vec{v}$ and s is $\pi - \eta^+_{i,j}$, the angle of friction needed is $\eta^+_{i,j} - \frac{\pi}{2}$. Thus, θ must be greater than $\max(\frac{\gamma_j}{2}, \eta^+_{i,j} - \frac{\pi}{2}, \eta^-_{i,j} - \frac{\pi}{2})$ for strategy two by picking one specific vertex of P.

By taking the minimum over all choices for C_j and the minimum of strategies one and two, the claim follows. □

Combining Lemmas 4 and 5 yields the following theorem.

Theorem 3. *Let P be a convex Polygon with vertices $C_0, \dots, C_{n-1}$ and angles $\gamma_0, \dots, \gamma_{n-1}$. If $\theta > \max_{0 \leq i < n} \left(\min_{j \in P_i} \left(\frac{\gamma_i}{2}, \max\left(\frac{\gamma_j}{2}, \eta^+_{i,j} - \frac{\pi}{2}, \eta^-_{i,j} - \frac{\pi}{2}\right)\right)\right)$, where $\eta^+_{i,j} := \sum_{C_k \in P^+_{i+1,j-1}} \delta_k$ and $\eta^-_{i,j} := \sum_{C_k \in P^-_{i-1,j+1}} \delta_k$, then every configuration of two particles can be reached.*

D. Reconfiguration of two particles in regular n-gons

Theorem 4. *If P is a regular polygon with n vertices and if $\mu > \cot(\pi/n)$, then every reconfiguration is possible.*

Proof. In a regular polygon, every inner angle is $\frac{n-2}{n}\pi$. We know that $\max\left(\frac{\gamma_j}{2}, \eta^+_{i,j} - \frac{\pi}{2}, \eta^-_{i,j} - \frac{\pi}{2}\right) \geq \frac{\gamma_j}{2} = \frac{n-2}{2n}\pi$ for every pair (i, j). Therefore, due to Theorem 3, $\theta > \frac{n-2}{2n}\pi$ is sufficient to cover the whole Δ configuration, and we can guarantee every configuration of two particles. Thus, the coefficient of friction is $\mu = \tan(\theta) > \tan(\frac{n-2}{2n}\pi) = \cot(\frac{\pi}{n})$. □

IV. Reconfiguration of Many Particles

In this section, we consider more than two particles. We show further limitations by demonstrating that not every reconfiguration of three particles may be possible. On the positive side, we show that we can perform arbitrary permutations for a line of n particles.

Theorem 5. *Consider the class $\mathscr{C}$ of configurations of three particles in a square, where one of the particles lies within the bounding rectangle of the other two particles. If $\theta > \frac{\pi}{2}$, then we can reconfigure any configuration to any configuration of $\mathscr{C}$. Furthermore, $\mathscr{C}$ contains $\frac{1}{3}$ of all possible configurations.*

Proof. W.l.o.g., let r_1, r_2 and r_3 be the three particles such that the x- and y-coordinates in the goal configuration are monotonically increasing, i.e., $r_1.x \leq r_2.x \leq r_3.x$ and $r_1.y \leq r_2.y \leq r_3.y$. We can also assume that the same holds for the x-coordinates in the start configuration (or else we start using the swap strategy from the last section). Proceed as follows: (1) Move r_1 to the lower left corner of the square and (2) use zig-zag moves to move r_3 to the top right corner. Then, (3) we can use zig-zag moves to move r_2 to a position, such that r_1 and r_2 have the same relative position as in the goal configuration. (4) Translate r_1 together with r_2 such that r_2 and r_3 have the correct relative position. As a last step (5) we can translate all three particles to the desired goal configuration.

To show that this strategy is correct, we show that we can carry out all five steps. We can do step (1) by simply translating all particles. We show that we can do step (2) in the previous section. For step (3), assume that we move r_2 further away from r_1. This means the zig-zag moves cannot affect r_3. Due to the angle of friction of $\theta > \frac{\pi}{2}$ we can move r_2 without moving r_1. Step (4) and (5) are simple translations and can therefore be performed.

Now, it is left to show that $\mathscr{C}$ contains $\frac{1}{3}$ of all configurations. There are 12 choices for the two particles that define the bounding rectangle and for a fixed choice these are

$$\int_0^1 \int_0^1 \int_0^{x_1} \int_0^{y_1} (x_1 - x_2)(y_1 - y_2)\, \mathrm{d}y_2 \mathrm{d}x_2 \mathrm{d}y_1 \mathrm{d}x_1 = \frac{1}{36}$$

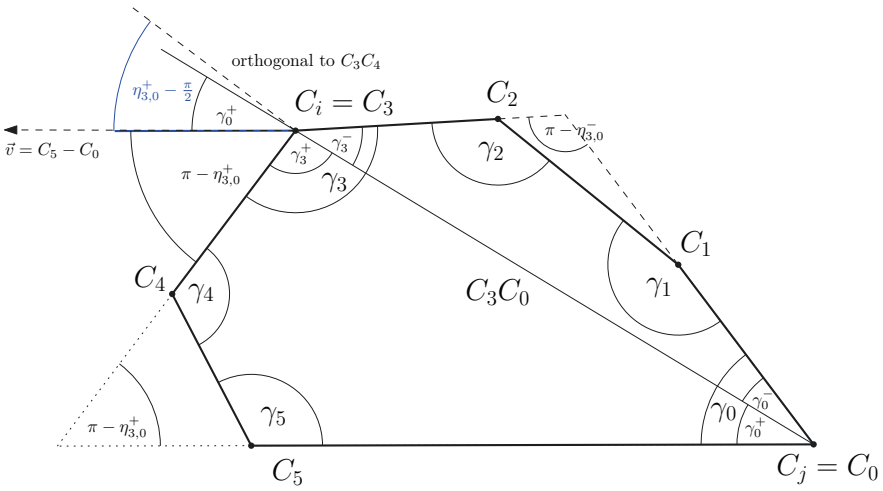

Fig. 9. Second strategy to cover the C_i-area (Lemma 5). Assuming one particle in C_3 and one particle in C_0. Blue angle is sufficient as angle of friction to reach any position in $P^+_{3,0} = C_3C_4C_5C_0$ with the particle in C_0 without moving the particle in C_3.

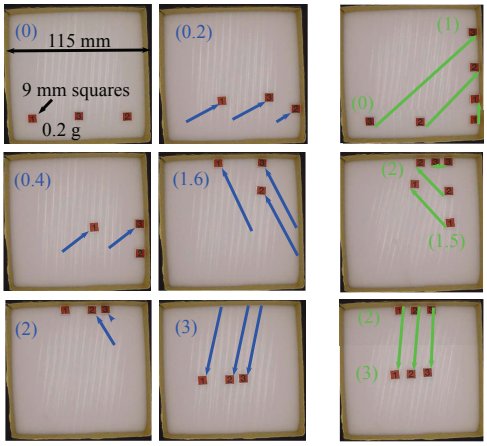

Fig. 10. Sorting multiple particles (hardware experiments, see video attachment [15]). In blue (1,3,2)→(1,2,3). In green (3,2,1)→(1,2,3). All particles move when commanded, unless friction with the boundary prevents motion. Boundary is coated with 220 grit sandpaper, giving $\theta_B = 20.2° \pm 2.22°$ and the acetal floor $\theta_F = 55.4° \pm 4.9°$.

of all configurations. Therefore, in total $\mathscr{C}$ contains $\frac{1}{3}$ of all configurations. □

Theorem 6. *There are configurations of three particles in a square we cannot reach, unless we have infinite friction.*

Proof. Consider the goal configuration with particle r_1 in the top left corner, particle r_2 in the bottom left corner, and particle r_3 in the middle of the right side of the square. Assume r_1 is the last particle reaching the goal position (or together with the other particles). Then, the last moving direction would also move r_3 away from its goal position. Therefore, the assumption is wrong. The same holds for particle r_2. If r_3 is the last particle reaching the goal position, then any of the last moving direction would also move r_1 or r_2 away from their goal position. Because no particle can be the last particle reaching its goal position, we can not reach the desired goal configuration. □

Theorem 7. *Consider n particles in a square with distance d between adjacent particles. If the angle of friction $\theta > \frac{\pi}{4}$ then we can reorder the particles.*

Proof. Consider some permutation Π of the particles. The idea is to move the $\Pi(n-i)$-th particle to the left side of the current line in round i, thus performing a mix of selection sort and insertion sort.

Assume the line lies horizontally within the square. Then we push the line to the left until the first particle hits the wall. We start to move all particles with a diagonal down-left movement (see Fig. 11(a)). This only moves particles that are not placed on a wall. We stop the movement when the $\Pi(n-i)$-th particle p hits the wall (see Fig. 11(b)). After translating all particles such that p gets trapped in the lower left corner, we perform a diagonal right-down movement until the former left neighbor of p has position $(\frac{d}{2}, \frac{d}{2})$ (see Fig. 11(c)). Then, we move all particles except p with zig-zag moves to the top wall, where we can rebuild a line of $n-1$ particles by repeating top-right, down-left, and zig-zag moves (see Fig. 11(d)-(f)). With simple translations we can add p to the left side with distance d. Therefore, after i repetitions of this strategy, the left i particles of the current line are sorted in ascending order. □

See Figure 10 for a real-world demonstration of these arguments, showing their practical usefulness.

V. Hardware Experiments

To show the practical usefulness of our theoretical work, we built 2D workspaces containing two sliders, with gravity as external force. The workspace was tilted by a robot arm. See our video [15] for animation and explanations.

A. Hardware platform and workspace

The triangular workspace has side walls of length {270,198,126} mm. Our workspace floor was made of nonstick teflon oven liners and the boundary walls were made of laser-cut acrylic. The pentagonal particles are laser-cut acrylic with side lengths of 3 mm with teflon tape on their underside.

The workspace is held by the gripper of a UR-3 robotic arm. The 4th and 6th joints are used to tilt the workspace in arbitrary directions, with the 5th joint oriented at 90°.

The first sections of this paper assumed a single, constant coefficient of friction of μ, where $\mu \in [0, \infty]$. A particle slides if the workspace is tilted beyond the angle $\arctan(\mu)$. The wall's coefficient of static friction (acrylic on acrylic) is approximately $\mu_w = 0.61$ $(\theta = 31.4°)$ (measured by placing the particle on this surface and tilting until the particle first slides). The floor's coefficient of static friction (teflon tape on teflon oven liner) is approximately $\mu_f = 0.207$ $(\theta = 11.7°)$.

The composite force of static friction is a function of table tilt. The force causing the particle to slide is opposed by the static friction with the floor and with the wall.

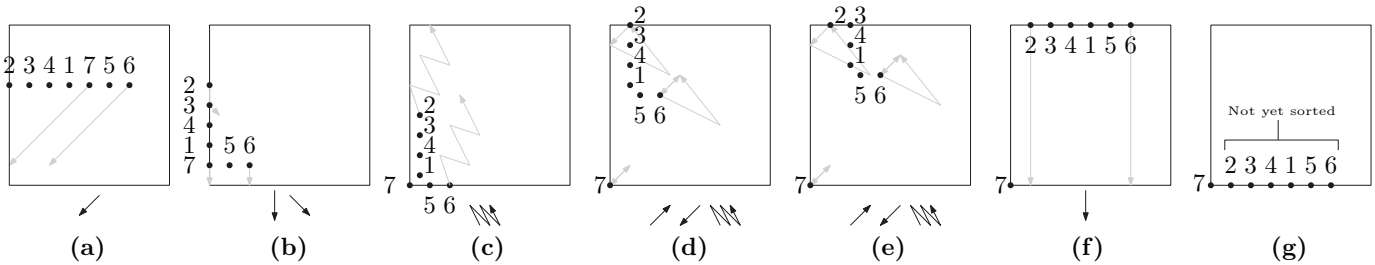

Fig. 11. First iteration of the sorting strategy. Arrows beneath the square indicate the moves used to reach the next configuration. Gray arrows indicate trajectories for particles 2, 6 and 7. (a): A line with desired ordering. (b),(c): Extracting largest number. (d)-(f): Rebuilt line with remaining particles. (g): Add particle to line.

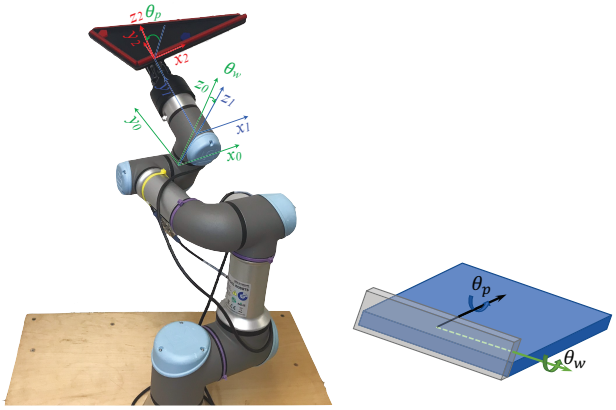

Fig. 12. The workspace (black triangle) is tilted by the fourth and sixth links of a UR-3 robot. The workspace walls have a higher coefficient of friction than the workspace floor.

B. Model for wall and floor friction

Any tilt of a 2D workspace can be described by first a tilt θ_w about the axis parallel to the boundary wall (such that positive θ_w slopes the workspace toward the wall), followed by a tilt θ_p about the axis perpendicular to the first tilt and the original gravity axis.

We can therefore first apply a rotation about the world gravity axis (the z-axis) to align the boundary wall with the world x-axis, rotate θ_w about the current x-axis, and rotate θ_p about the current y-axis to complete the composite tilt. The composite rotation is

$$R_{z,\phi}R_{x,\theta_w}R_{y,\theta_p} = R_{z,\phi}\begin{bmatrix} c_{\theta_p} & 0 & s_{\theta_p} \\ s_{\theta_w}s_{\theta_p} & c_{\theta_w} & -c_{\theta_p}s_{\theta_w} \\ -c_{\theta_w}s_{\theta_p} & s_{\theta_w} & c_{\theta_w}c_{\theta_p} \end{bmatrix}. \quad (1)$$

Here we use the shorthand $\sin(x) = s_x$ and $\cos(x) = c_x$. For simplicity, the following analysis will ignore the initial rotation about the z-axis. The third row describes how the components of the original gravity vector are distributed along the boundary wall ($-c_{\theta_w}s_{\theta_p}$), perpendicular to the wall (s_{θ_w}) and into the floor ($c_{\theta_w}c_{\theta_p}$). For simplicity, assume the force of gravity on the particle is 1N: $f_g = [0, 0, -1]^\top$. To contact the floor, both θ_w and θ_p must have magnitude less than $\pi/2$. The normal force from the tilted floor is $f_{\text{N,floor}} = c_{\theta_w}c_{\theta_p}$. If a particle is touching a wall *and* the tilt $\theta_w > 0$ and thus pushes the particle against the wall, then the wall generates a normal force

$$f_{\text{N,wall}} = \begin{cases} s_{\theta_w}, & \theta_w > 0 \\ 0, & \text{else.} \end{cases} \quad (2)$$

The force after accounting for the normal force is

$$f_{\text{slide}} = f_g - f_{\text{N,floor}} - f_{\text{N,wall}}. \quad (3)$$

The static friction force is proportional to the normal force. The particle will only slide if f_{slide} is greater than the static friction force, i.e.,

$$|f_{\text{slide}}| > \mu_f |f_{\text{N,floor}}| + \mu_w |f_{\text{N,wall}}|. \quad (4)$$

The particle slides if the following quantity is positive:

$$\begin{cases} |c_{\theta_w}s_{\theta_p}| - \mu_f c_{\theta_w}c_{\theta_p} - \mu_w s_{\theta_w} & \theta_w > 0 \\ \sqrt{1 - c_{\theta_w}^2 c_{\theta_p}^2} - \mu_f c_{\theta_w}c_{\theta_p} & \text{else} \end{cases}. \quad (5)$$

a) Conversion to rotation about x and y axes: The two-links of our robot generate a rotation about the global x-axis, followed by a rotation about the current y-axis: $R_{x,\theta_x}R_{y,\theta_y}$. To generate the appropriate gravitational force described by a z rotation of ϕ followed by θ_w about the wall and θ_p perpendicular to the wall, we only need to reproduce the third column of (1), and select

$$\theta_y = \arcsin\left(c_\phi s_{\theta_p} + c_{\theta_p}s_{\theta_w}s_\phi\right) \quad (6)$$

$$\theta_x = \arcsin\left(\frac{s_{\theta_w}c_{\theta_p}c_\phi - s_{\theta_p}s_\phi}{c_{\theta_y}}\right) \quad (7)$$

b) Verification of model: The slipping force from (5) is the left plot of Fig. 13. Particles not touching a wall slip outside the green circle; particles touching a wall only slip in the region below the red line. The required angle of friction to avoid slipping is shown in the left plot of Fig. 13.

$$\text{Angle of Friction} = \frac{\pi}{2} - \arctan(s_{\theta_p}c_{\theta_w}, s_{\theta_w}) \quad (8)$$

C. Demonstration: placing particles in opposite corners of a triangular workspace

For this demonstration, two pentagonal particles positions were placed into opposing corners of a triangle. A motion sequence using the blue strategy from Section III was used to hold one particle in the left corner while the other was moved to the right side. Then the red strategy was used to swap the particle's positions. Repeating the procedure iterates between placing the particles in opposite corners every 36 moves using the procedure. Representative screenshots of a rearrangement procedure are shown in Fig. 14. The tilt used to move both particles were $(\theta_w, \theta_p) = (0°, 20°)$, shown in Fig. 13 by a blue point. The particles both move, since this

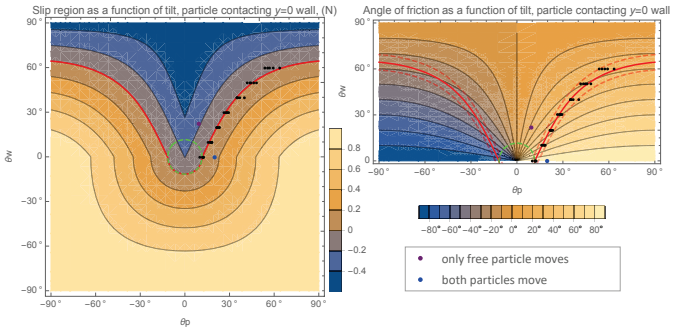

Fig. 13. (Left) Contour plot showing slipping force due to gravity minus static friction forces from the wall and floor. Regions with positive values will slip. Particles not at a wall will slip outside the green circle and particles at the wall will slip below the red line. (Right) Contour plot showing angle of friction. The 35 data points overlaid show where components slipped, as a function of tilt about the wall θ_w and perpendicular to the wall θ_p. The experiments moved both particles using the tilt marked by the blue point, and the purple point moved only the free particle.

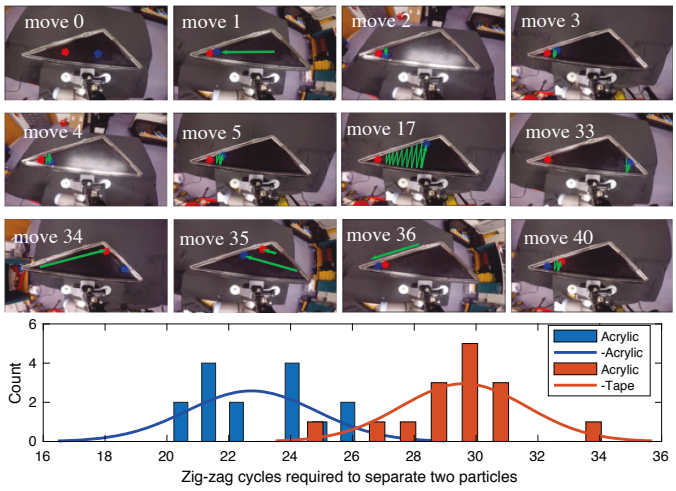

Fig. 14. (top) Two pentagonal particles were placed into opposing corners of a triangle, and their positions are switched every 36 moves using the procedure from Section III (see video attachment https://youtu.be/hSa4EmjHXAI) [15]. (bottom) Histogram data on required number of zigzag movements required for two combinations of wall and particle materials.

would require an angle of friction of $90°$. To move one particle we used $(\theta_w, \theta_p) = (22°, 9.5°)$, shown in Fig. 13 by a purple point, which had an angle of friction of $22.2°$. The tilts were performed at $66°/s$.

To measure the repeatability of this setup, we counted the number of zigzag cycles required to move one particle from touching the first particle in the left corner to touching the opposite triangle corner while the first particle stays stationary. Figure 14 shows a normal distribution fit to counts from 15 trials for two different boundary materials: acrylic and electrical tape over acrylic. When the particle impacts an acrylic boundary, it tends to slide along the edge, resulting in less required cycles than if the boundary is covered with electrical tape. We reject the null hypothesis that the different surfaces require the same number of cycles with p-value 6.7×10^{-10}.

VI. Conclusion

We introduced a novel approach for rearranging the positions of particles by applying global uniform forces, making use of different local static friction to achieve arbitrary goal positions. We provided strategies enabling arbitrary rearrangements of two particles in a triangle, giving a characterization of the critical coefficient of friction in terms of the boundary geometry. These results are extended to convex polyominoes, and for rearranging larger numbers of particles, and employed for practical experiments. Future work can now investigate optimal motion planning (shortest paths, reproducibility, throughput), as well as coupling these results with orientation control and possible applications in part assembly.

References

[1] S. Akella, W. H. Huang, K. M. Lynch, and M. T. Mason, "Parts feeding on a conveyor with a one joint robot," *Algorithmica*, vol. 26, no. 3-4, pp. 313–344, 2000.

[2] G. Aloupis, J. Cardinal, S. Collette, F. Hurtado, S. Langerman, and J. O'Rourke, "Draining a polygon—or—rolling a ball out of a polygon," *Computational Geometry*, vol. 47, no. 2, pp. 316–328, 2014.

[3] D. Arbuckle and A. A. Requicha, "Self-assembly and self-repair of arbitrary shapes by a swarm of reactive robots: algorithms and simulations," *Autonomous Robots*, vol. 28, no. 2, pp. 197–211, 2010.

[4] J. Balanza-Martinez, A. Luchsinger, D. Caballero, R. Reyes, A. A. Cantu, R. Schweller, L. A. Garcia, and T. Wylie, "Full tilt: Universal constructors for general shapes with uniform external forces," in *SODA*, 2019, pp. 2689–2708.

[5] A. Becker, E. D. Demaine, S. P. Fekete, and J. McLurkin, "Particle computation: Designing worlds to control robot swarms with only global signals," in *IEEE ICRA*, 2014, pp. 6751–6756.

[6] A. T. Becker, E. D. Demaine, S. P. Fekete, J. Lonsford, and R. Morris-Wright, "Particle computation: complexity, algorithms, and logic," *Natural Computing*, vol. 18, no. 1, pp. 181–201, 2019.

[7] A. T. Becker, S. P. Fekete, P. Keldenich, D. Krupke, C. Rieck, C. Scheffer, and A. Schmidt, "Tilt assembly: algorithms for micro-factories that build objects with uniform external forces," *Algorithmica*, pp. 1–23, 2017.

[8] M. A. Erdmann and M. T. Mason, "An exploration of sensorless manipulation," *IEEE J. Robot. Autom.*, vol. 4, no. 4, pp. 369–379, 1988.

[9] K. Y. Goldberg, "Orienting polygonal parts without sensors," *Algorithmica*, vol. 10, no. 2-4, pp. 201–225, 1993.

[10] P. S. S. Kim, A. T. Becker, Y. Ou, A. A. Julius, and M. J. Kim, "Imparting magnetic dipole heterogeneity to internalized iron oxide nanoparticles for microorganism swarm control," *Journal of Nanoparticle Research*, vol. 17, no. 3, pp. 1–15, 2015.

[11] J. S. Lewis and J. M. O'Kane, "Planning for provably reliable navigation using an unreliable, nearly sensorless robot," *Int J Robot Res.*, vol. 32, no. 11, pp. 1342–1357, 2013.

[12] K. M. Lynch and M. T. Mason, "Stable pushing: Mechanics, controllability, and planning," *Int J Robot Res.*, vol. 15, no. 6, pp. 533–556, 1996.

[13] P. Mannam, A. V. Volkov, R. Paolini, G. Chirikjian, and M. T. Mason, "Sensorless pose determination using randomized action sequences," *Entropy*, vol. 21, no. 2, p. 154, 2019.

[14] M. Rubenstein, C. Ahler, N. Hoff, A. Cabrera, and R. Nagpal, "Kilobot: A low cost robot with scalable operations designed for collective behaviors," *Robotics and Autonomous Systems*, vol. 62, no. 7, pp. 966–975, 2014.

[15] A. Schmidt, V. M. Baez, A. T. Becker, and S. P. Fekete, "Particle relocation," 2019. [Online]. Available: https://youtu.be/hSa4EmjHXAI

[16] A. Schmidt, S. Manzoor, L. Huang, A. T. Becker, and S. P. Fekete, "Efficient parallel self-assembly under uniform control inputs," *IEEE RA-L*, vol. 3, no. 4, pp. 3521–3528, 2018.

[17] S. Shahrokhi, A. Mahadev, and A. T. Becker, "Algorithms for shaping a particle swarm with a shared input by exploiting non-slip wall contacts," in *IEEE/RSJ IROS*, 2017, pp. 4304–4311.

[18] S. Shahrokhi, J. Shi, B. Isichei, and A. T. Becker, "Exploiting nonslip wall contacts to position two particles using the same control input," *IEEE Trans. Robot.*, pp. 1 – 12, 2019.

[19] Y. Zhang, X. Chen, H. Qi, and D. Balkcom, "Rearranging agents in a small space using global controls," in *IEEE/RSJ IROS*, 2017, pp. 3576–3582.

[20] Y. Zhang, E. Whiting, and D. Balkcom, "Assembling and disassembling planar structures with divisible and atomic components," *IEEE Trans. Autom. Sci. Eng.*, vol. 15, no. 3, pp. 945–954, 2018.